Active hydrogen species on TiO_2 for photocatalytic H_2 production†

Zongfang Wu,‡[a] Wenhua Zhang,‡[b] Feng Xiong,[a] Qing Yuan,[a] Yuekang Jin,[a] Jinlong Yang[a] and Weixin Huang*[ab]

Photocatalytic H_2 production over TiO_2 has attracted tremendous attention and achieved great progress, but the active hydrogen species is still unknown. Employing a rutile $TiO_2(110)$ surface as a model catalyst we report here for the first time the direct observation of photocatalytic H_2 production under ultrahigh vacuum conditions during UV-light irradiation at 115 K and the identification of negatively-charged hydride-type H-Ti species as the corresponding photoactive surface species by means of thermal desorption spectroscopy, photon-stimulated desorption spectroscopy, X-ray photoelectron spectroscopy and DFT calculations. The formation and stability of H-Ti species are closely related to available surplus electrons on the rutile $TiO_2(110)$ surface that can be created by the formation of surface BBO vacancies or by the formation of surface hydroxyls *via* the adsorption of atomic H or molecular H_2 on O sites. The photocatalytic H_2 production from H-Ti species is hole-mediated and co-existing water exerts a negative effect on this process.
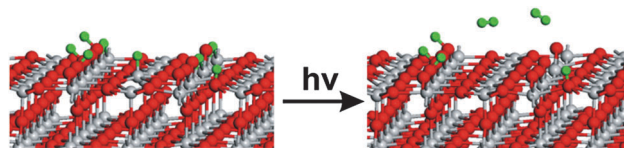
Introduction

TiO_2-based photocatalysis has grown into a fascinating research field since Fujishima and Honda's first reports of UV-light-induced redox chemistry on TiO_2.[1] Consequently, the fundamental studies of photochemistry of the TiO_2 surface largely employing a rutile $TiO_2(110)$ surface as the prototypical model surface have been performed.[2] Insights have been recently achieved into the photochemistry of several important molecules involved in photocatalytic reactions, such as O_2,[3] CO,[4] methanol[5–7] and H_2O.[8] However, little progress has been made on the fundamental understanding of photocatalytic H_2 production, the core issue in photocatalysis. The commonly observed and most investigated hydrogen adatoms on the rutile $TiO_2(110)$ surface are bridging hydroxyls ($O_{BBO}H$) that can be prepared by a number of methods,[9,10]

Scheme 1 Schematic illustration of photocatalytic H_2 production from hydride-type H-Ti species on the rutile $TiO_2(110)$ surface. Red, grey and green balls, respectively, represent O, Ti and H atoms.

but the $O_{BBO}H$ species was proven to be not photoactive.[10] Other proposed types of hydrogen adatoms include subsurface hydroxyls[9d,11] and hydride-type H-Ti species,[9b,12] and their photo-activities have not been reported. In this paper we studied the surface chemistry and photochemistry of various types of hydrogen species on the rutile $TiO_2(110)$ surface generated by adsorption of gas-phase atomic hydrogen at 115 K using thermal desorption spectroscopy (TDS), photon-stimulated desorption spectroscopy (PSD), X-ray photoelectron spectroscopy (XPS) and DFT calculations. Photocatalytic H_2 production on a rutile $TiO_2(110)$ surface at 115 K was for the first time observed and a negatively-charged hydride-type H-Ti species was identified as the photoactive surface species (Scheme 1).

Experimental and theoretical calculation details

All experiments were performed in a Leybold stainless-steel ultrahigh vacuum (UHV) chamber with a base pressure of 5×10^{-11} mbar.[7d]

[a] *Hefei National Laboratory for Physical Sciences at Microscale, Suzhou Nano Tech Co-innovation Center and Department of Chemical Physics, University of Science and Technology of China, Hefei 230026, China. E-mail: huangwx@ustc.edu.cn*

[b] *CAS Key Laboratory of Materials for Energy Conversion and Department of Materials Science and Engineering, University of Science and Technology of China, Hefei 230026, China*

This journal is © the Owner Societies 2014

Phys. Chem. Chem. Phys., 2014, **16**, 7051–7057 | 7051

The UHV chamber was equipped with facilities for X-ray photoelectron spectroscopy, ultraviolet photoelectron spectroscopy, low energy electron diffraction, and differential-pumped quadrupole mass spectrometry. The rutile $TiO_2(110)$ single crystal purchased from MaTeck was mounted onto a Ta support plate (1 mm thick and of the same dimensions as the crystal) using a high temperature alumina-based inorganic adhesive (Aremco 503) and graphite powder (99.9995%, Alfa Aesar China Co., Ltd). The Ta support was cooled and resistively heated by two Ta wires spot-welded to its backside. The sample temperature could be controlled between 100 and 1273 K and was measured using a chromel–alumel thermocouple spot-welded to the backside of the sample. Prior to experiments, the rutile $TiO_2(110)$ sample was cleaned by repeated cycles of Ar ion sputtering, oxidation and annealing at 1000 K for 10 min until LEED gave a sharp (1 × 1) diffraction pattern and no contaminants could be detected by XPS. The reproducible preparation of the clean rutile $TiO_2(110)$ surface was verified by means of CO and CO_2 TDS experiments.

D_2O (D > 99.9%, SIGMA-ALDRICH) and H_2O (>18 MΩ) were purified by repeated freeze–pump–thaw cycles. D_2 (>99.999%, Nanjing ShangYuan Industry Factory), CO (>99.99%, Nanjing ShangYuan Industry Factory) and CO_2 (>99.99%, Nanjing ShangYuan Industry Factory) were used as received. The purity of all reactants was checked by QMS prior to experiments. The exposure of atomic hydrogen (deuterium) was accomplished using a MGC75 thermal gas cracker with an Ir capillary. All exposures were reported in Langmuir (1 L = 1.0×10^{-6} Torr s) without corrections for the gauge sensitivity. During the TDS measurements, the sample was positioned ~1 mm away from a collecting tube of a differential-pumped QMS and the heating rate was 2 K s^{-1}. XPS spectra were recorded using Mg Kα radiation ($h\nu$ = 1253.6 eV) with a pass energy of 20 eV.

UV irradiation was accomplished using a 100 W Hg arc lamp (Oriel 6281) which provided a pressure-broadened emission spectrum from gaseous Hg with significant intensity in the UV-light region. A water filter was used to remove the IR portion of the emission spectrum. The UV-light was focused onto the tip of a single strand, a 0.6 mm diameter fused silica fiber optic cable that directed the light through a UHV-compatible feed-through onto the rutile $TiO_2(110)$ face without exposure to extraneous surfaces. Due to our UHV system set-up, the distance between the sample and the differential-pumped QMS during PSD measurements was much longer than that during TDS measurements. This resulted in a weaker QMS signal in PSD experiments than in TDS experiments. Exposure of the $TiO_2(110)$ crystal at 115 K to the UV-light resulted in the increase of crystal temperature by no more than 3 K.

DFT calculations were performed employing the computational code Vienna Ab initio simulation package (VASP).[13] The Perdew–Burke–Enzerhof (PBE)[14] functional was adopted. For energy calculations, plane wave basis sets with an energy cutoff of 450 eV were adopted. The rutile $TiO_2(110)$ surface was modeled using five O–Ti–O layers and a (2 × 2) supercell and (2 × 6 × 1) grid were used. The adsorption energy E_{ads} was calculated as $E_{ads} = E_{nH(a)/TiO_2} - (nE_{H(g)} + E_{TiO_2})$, where $E_{nH(a)/TiO_2}$,

$E_{H(g)}$ and E_{TiO_2}, respectively, represent the energy of H adatoms on rutile $TiO_2(110)$, atomic H and clean rutile $TiO_2(110)$, and n represents the number of H adatoms. The charge accumulated on H adatoms was analyzed using the Bader charge analysis.[15]

Results and discussion

No desorption trace was observed from the rutile $TiO_2(110)$ surface after an exposure of 1000 L D_2 at 115 K (Fig. S1A, ESI†), suggesting that molecular D_2 does not adsorb on the rutile $TiO_2(110)$ surface under UHV conditions. However, after an exposure of 50 L atomic D at the same temperature, desorption traces of D_2, HD, D_2O, HDO and H_2O were observed in the TDS spectra (Fig. 1A). A sharp D_2 desorption feature was observed at the on-set edge of D_2 desorption trace. Such a feature was not observed in the corresponding HD desorption trace. This indicates that it should arise from molecularly-adsorbed $D_2(a)$ species. Meanwhile this feature was also not observed in our previous TDS measurements after exposure of atomic D on FeO(111)/Pt(111) in the same UHV system.[16] A unique design of the sample assembly for rutile $TiO_2(110)$ was the use of a Ta plate to ensure the heating of the semiconductor $TiO_2(110)$ sample as homogeneously as possible. Therefore we attributed the sharp D_2 desorption feature at the on-set edge to molecularly-chemisorbed D_2 on the Ta plate. This is also supported by the observation of this feature after the sample was exposed to 1000 L D_2 at 115 K (Fig. S1A, ESI†). Except the desorption trace of molecularly-chemisorbed D_2 from the Ta plate, three HD/D_2 desorption features were observed in the TDS spectra, a major desorption peak at 207 K (denoted as α) and two shoulders at 300 and 160 K (respectively denoted as β and γ). It was previously reported that $O_{BBO}H$ on the rutile $TiO_2(110)$ surface with bridge-bonded oxygen vacancies could react to produce H_2 above 400 K.[9d,10b] We also measured TDS spectra after an exposure of 50 L D on the rutile $TiO_2(110)$ surface at 320 K (Fig. 1B). A D_2 desorption peak evolves above 500 K and could be attributed to the reaction between $O_{BBO}H$. Therefore, the low-temperature α, β and γ HD/D_2 desorption features should not result from the reaction between $O_{BBO}H$ on the rutile $TiO_2(110)$ surface. These results suggest that adsorption

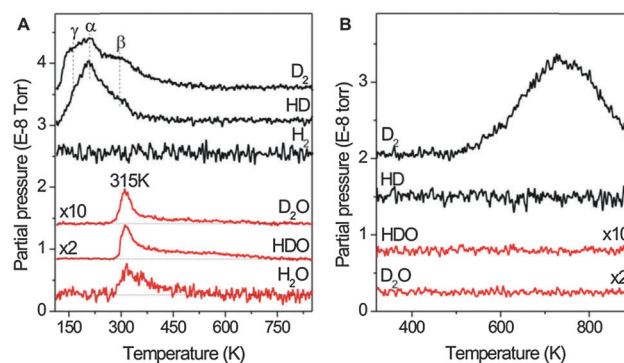Fig. 1 TDS spectra after the rutile $TiO_2(110)$ surface was exposed to 50 L atomic D at (A) 115 K and (B) 320 K.

7052 | *Phys. Chem. Chem. Phys.*, 2014, **16**, 7051–7057

This journal is © the Owner Societies 2014

of atomic D on the rutile TiO$_2$(110) surface at 115 K should open up novel low-temperature surface reactions to produce molecular HD/D$_2$.

The D$_2$O/HDO/H$_2$O desorption traces after an exposure of 50 L atomic D on the rutile TiO$_2$(110) surface at 115 K consist of a peak at 315 K and a weak and broad peak at ∼570 K. Comparing with corresponding TDS spectra after an exposure of 0.01 L D$_2$O on the rutile TiO$_2$(110) surface at 115 K (Fig. S2, ESI†), the peak at 315 K arises from the desorption of molecularly-chemisorbed water on Ti$_{5C}$ sites and that at ∼570 K from water produced by the reaction between O$_{BBO}$H. These observations agree with a previous report.[2b] Therefore exposure of high-energetic atomic D on the rutile TiO$_2$(110) surface at 115 K not only forms surface hydroxyls (H(g) + O$_{lattice}$ → O$_{lattice}$H) but also further abstracts surface lattice oxygen to produce molecularly-chemisorbed water (H(g) + O$_{lattice}$ → H$_2$O(a) + O$_{vacancy}$) accompanied by the creation of oxygen vacancies. When atomic D was exposed at 320 K no HDO/D$_2$O desorption trace was observed (Fig. 1B), although the formation of surface hydroxyls was indicated by the D$_2$ desorption feature. These results suggest the different reactivities of surface hydroxyls formed on the rutile TiO$_2$(110) surface by exposure of atomic D at 115 and 320 K. This could be attributed to the production and desorption of water during the exposure at 320 K that results in the accumulation of surface oxygen vacancies on the rutile TiO$_2$(110) surface. Our previous results demonstrate that the accumulation of surface oxygen vacancies on FeO(111)/Pt(111), Fe$_3$O$_4$(111)/Pt(111) and CeO$_2$(111)/Cu(111) will switch the reaction pathway of surface hydroxyls from the water formation to the H$_2$ formation.[16,17] The results about the influence of surface oxygen vacancies on the reactivity of hydroxyls on the rutile TiO$_2$(110) surface are out of the scope of this paper and will be reported elsewhere.

It is noteworthy that the HD and HDO desorption traces were always observed to respectively accompany D$_2$ and D$_2$O desorption traces in the TDS spectra when atomic D was exposed at 115 K. This was due to the H–D exchange reactions between D adatoms and OH/H$_2$O species formed by the adsorption of residual water in the UHV chamber on the rutile TiO$_2$(110) surface. When atomic D was exposed at 320 K, the temperature at which water could not adsorb, the H–D exchange reactions did occur and HD desorption trace was not observed to accompany the D$_2$ desorption trace (Fig. 1B).

Fig. 2A and B respectively show HD and D$_2$ TDS spectra from the rutile TiO$_2$(110) surface as a function of atomic D exposure at 115 K. The α peak dominates in both HD and D$_2$ TDS spectra at low atomic D exposures, and β and γ peaks gradually develop with the increase of the atomic D exposure. The HD and D$_2$ desorption peaks approach the saturation at an atomic D exposure of 20 L (Fig. 2C and D). In the corresponding D$_2$O/HDO/H$_2$O TDS spectra (Fig. S3, ESI†), their desorption traces are not obvious at low atomic D exposures but then grow fast and do not saturate under the investigated atomic D exposures.

The adsorption of atomic D on the rutile TiO$_2$(110) surface at 115 K was also studied by XPS. The formation of both surface hydroxyls and chemisorbed water with the O 1s binding energy, respectively, at 532.5 and 534.3 eV were identified from the O 1s
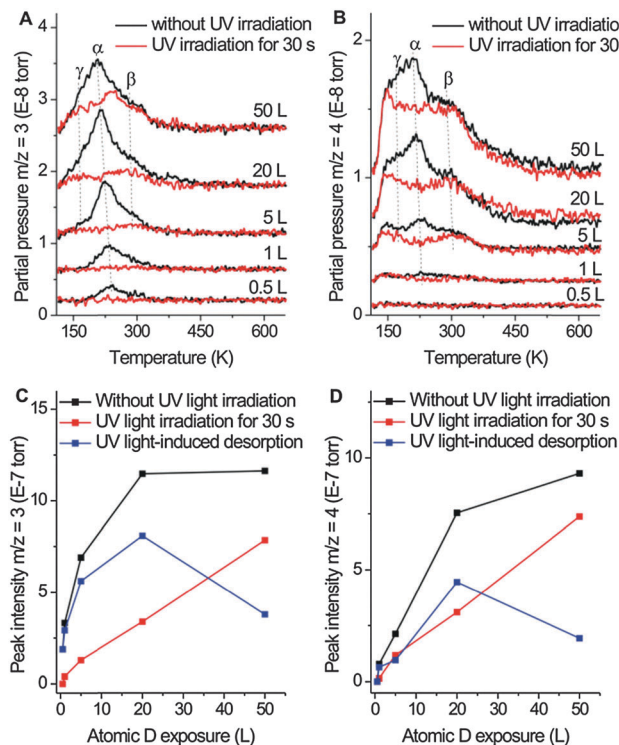

Fig. 2 (A) HD and (B) D$_2$ TDS spectra after the rutile TiO$_2$(110) surface was exposed to various exposures of atomic D at 115 K without and with subsequent UV light irradiation for 30 s, and integrating (C) HD and (D) D$_2$ TDS peak areas. The contribution of the sharp D$_2$ desorption feature from the Ta plate of the sample assembly was subtracted when integrating the D$_2$ TDS peak area (Fig. S1B and C, ESI†).

XPS difference spectra (Fig. S4, ESI†). When the rutile TiO$_2$(110) surface exposed to 20 L atomic D at 115 K was annealed, the O 1s feature of chemisorbed water disappeared between 270 and 330 K and that of surface hydroxyls disappeared before 700 K (Fig. S5, ESI†). These XPS results agree with the TDS results on the formation of surface hydroxyls and molecularly-chemisorbed water upon atomic D exposures on the rutile TiO$_2$(110) surface at 115 K and their subsequent desorption/reaction behaviours; however, we did not observe any XPS features that could be correlated with the α, β and γ molecular HD/D$_2$ desorption peaks in the TDS spectra. Therefore, adsorption of atomic hydrogen on the rutile TiO$_2$(110) surface at 115 K not only forms the common surface hydroxyls and water but also forms other types of hydrogen adatoms responsible for the H$_2$ production at low temperatures upon heating.

Rutile TiO$_2$(110) surfaces exposed to various exposures of atomic D at 115 K were then irradiated with UV light for 30 s at the same temperature, after which TDS spectra were taken. The HD/D$_2$ results are also included in Fig. 2, and the corresponding D$_2$O/HDO/H$_2$O results are shown in Fig. S6 (ESI†). The UV light irradiation strongly affects the HD/D$_2$ desorption features but not the D$_2$O/HDO/H$_2$O desorption features. Among the HD/D$_2$ desorption features, the α feature is most significantly affected by the UV light irradiation. After the UV light irradiation, it completely vanishes from the TDS spectra for the atomic D

exposures up to 20 L and substantially weakens in the TDS spectra for the atomic D exposure of 50 L. The γ feature is less affected by the UV light irradiation than the α feature, but its weakening upon UV light irradiation is evident in the TDS spectra. The β feature is seldom affected by the UV light irradiation, as it can be seen that the β HD/D_2 desorption peaks in the TDS spectra without and with the UV light irradiation are identical.

We also studied the influences of UV light irradiation on the desorption behaviours of other molecules on the rutile $TiO_2(110)$ surface including $D_2O/HDO/H_2O$, CO and CO_2, but did not observe any effects (Fig. S2 and S7, ESI†). During the UV light irradiation we observed a slight increase in the sample temperature of no more than 3 K. As shown in Fig. S7 (ESI†), the CO desorption feature from the rutile $TiO_2(110)$ surface occurring at lower temperatures than the α HD/D_2 desorption features is not affected by the slight increase in the sample temperature induced by UV light irradiation, and the α HD/D_2 desorption feature should not be affected either. Therefore, the disappearance/reduction of the α and γ HD/D_2 desorption peaks upon the UV light irradiation must result from the UV light irradiation-induced desorption of HD/D_2 from the rutile $TiO_2(110)$ surface at 115 K. These results demonstrate that H/D adatoms on the rutile $TiO_2(110)$ surface responsible for the α and γ HD/D_2 desorption peaks in the TDS spectra are photo-active for the photocatalytic H_2 production and that H/D adatoms responsible for the α HD/D_2 desorption peak are more active than those responsible for the γ HD/D_2 desorption peak. However, H/D adatoms on the rutile $TiO_2(110)$ surface responsible for the β HD/D_2 desorption peaks in the TDS spectrum are not photoactive. As shown in Fig. 2C and D, the photocatalytic HD/D_2 yields at 115 K initially increase with the atomic D exposure (the surface coverage of photoactive H/D adatoms) up to 20 L and then obviously drop with the further increase of atomic D exposure to 50 L. This infers that the efficiency of photocatalytic HD/D_2 production should decrease a lot with the increase of atomic D exposure from 20 to 50 L because the HD/D_2 TDS peaks saturate after the exposure of 20 L atomic D and thus the surface coverages of photoactive H/D adatoms after 20 and 50 L atomic D exposures are the same.

The UV light irradiation-induced desorption of HD/D_2 from the rutile $TiO_2(110)$ surface at 115 K was directly observed by PSD spectroscopy (Fig. 3A and B). Both HD and D_2 signals in the gas phase increased as soon as the UV light irradiation was on, unambiguously proving the occurrence of photocatalytic HD/D_2 production on the rutile $TiO_2(110)$ surface at 115 K. No other species was observed to be produced in the gas phase during the UV light irradiation. The photocatalytic HD/D_2 yields measured in the PSD spectra (Fig. 3C) initially increase with the atomic D exposure up to 20 L and then greatly drop with the further increase of the atomic D exposure to 50 L, consistent with corresponding TDS results (Fig. 2C and D). The weaker intensity of HD/D_2 in the PSD spectra than in the TDS spectra was due to our UHV system set-up described in the previous section.

Fig. 3A and B also show that the photocatalytic HD/D_2 reactions actually cease after a UV light irradiation time of ~15 s. This is
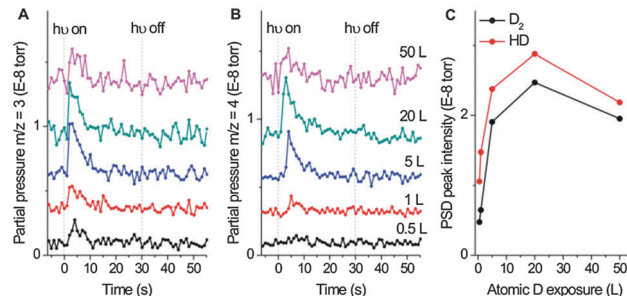

Fig. 3 (A) HD and (B) D_2 PSD spectra during 30 s UV light irradiation of the rutile $TiO_2(110)$ surface exposed to various exposures of atomic D at 115 K, and (C) integrating HD and D_2 PSD peak areas.

further confirmed by the comparative TDS and PSD results of the rutile $TiO_2(110)$ surface exposed to 50 L atomic D at 115 K followed by the UV light irradiation for different times (Fig. 4). The UV light irradiations for 30 and 300 s result in almost identical HD/D_2 TDS and PSD spectra whereas the UV light irradiation for 2 s results in stronger α and γ features in the HD/D_2 TDS spectra and lower HD and D_2 yields in the HD/D_2 PSD spectra. Interestingly the photocatalytic HD/D_2 productions were still observed even after the UV light irradiation for 2 s ceased. Similar results were also observed for an atomic D exposure of 5 L (Fig. S8, ESI†). This indicates that the charge-participated surface reaction occurs much later than the light absorption and charge generation processes in the photocatalytic H_2 production on the rutile $TiO_2(110)$ surface. This is reasonable because the light absorption and charge generation processes mostly occur in the bulk of rutile $TiO_2(110)$ and the generated
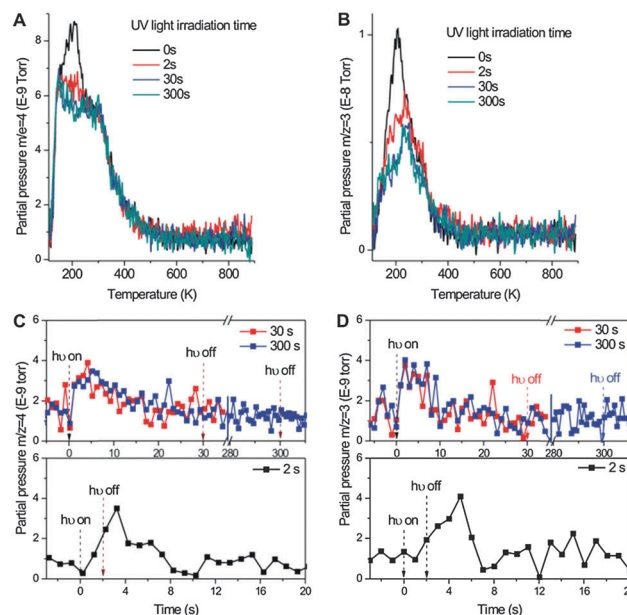

Fig. 4 (A) D_2 and (B) HD TDS spectra after the rutile $TiO_2(110)$ surface was exposed to 50 L atomic D at 115 K and then irradiated with UV light irradiation for different times. (C) D_2 and (D) HD PSD spectra after the rutile $TiO_2(110)$ surface was exposed to 50 L atomic D at 115 K and then irradiated with UV light irradiation for different times.

charges need to migrate from the bulk to the surface to participate in the surface reactions.

The above experimental results demonstrate that hydrogen adatoms other than surface hydroxyls formed upon adsorption of atomic hydrogen on the rutile $TiO_2(110)$ surface at 115 K not only facilely produce H_2 at low temperatures upon heating but also photocatalytically produce H_2 under the UV light irradiation at 115 K. These results represent the first experimental observation of photocatalytic H_2 production on the rutile $TiO_2(110)$ surface under UHV conditions. Besides $O_{BBO}H$ species, other proposed types of hydrogen adatoms on the rutile $TiO_2(110)$ surface include subsurface hydroxyls[9d,11] and hydride-type H-Ti species.[9b,12] The presence of subsurface hydroxyls and H-Ti species was also proposed on other rutile TiO_2 single crystal surfaces.[18] Subsurface hydroxyl species on TiO_2 was reported to be formed by the diffusion of hydrogen adatoms in $O_{BBO}H$ to the subsurface region at high temperatures[9d,18a] or by the tip manipulation process,[11] thus it cannot be formed under our experimental conditions. The presence of H-Ti species was previously indicated by a combined STM and electron stimulated desorption (ESD) study of the rutile $TiO_2(110)$ surface exposed to atomic hydrogen at 300 K[9b] and a low-energy ion scattering spectroscopy study of a highly defective sputtered rutile $TiO_2(110)$ surface exposed to 50 eV hydrogen ions at 300 K.[12] Previous theoretical calculation results reported that a H-Ti species was feasible to form together with $O_{BBO}H$ from atomic H adsorption and molecular H_2 dissociation on the stoichiometric rutile $TiO_2(110)$ surface but it was not so stable as $O_{BBO}H$.[9d,19] We thus proposed the hydride-type H-Ti species on the rutile $TiO_2(110)$ surface as the active hydrogen adatoms responsible for both low-temperature H_2 production upon heating and photocatalytic H_2 production.

Our results demonstrate that exposure of atomic H on the rutile $TiO_2(110)$ surface at 115 K forms the photoactive hydride-type H-Ti species. DFT calculations were performed to understand the relevant microscopic pictures. Different from previous DFT studies only involving stoichiometric rutile $TiO_2(110)$ surfaces,[9d,19] we calculated the adsorption of atomic H on both stoichiometric and defective rutile $TiO_2(110)$ surfaces. Surface oxygen vacancies should be always present on the rutile $TiO_2(110)$ surface exposed to atomic H due to the formation of water. Meanwhile the formation of H-Ti species was only observed on a highly defective sputtered rutile $TiO_2(110)$ surface exposed to 50 eV hydrogen ions at 300 K but not on the stoichiometric surface.[12] Therefore it is necessary to consider the effect of oxygen vacancies on the adsorption of atomic H on the rutile $TiO_2(110)$ surface.

Fig. 5 illustrates likely adsorption sites for atomic H on the (2×2) rutile $TiO_2(110)$ surface with one BBO vacancy (θ_{Ov} = 0.25 ML). On the stoichiometric surface, a H atom adsorbs strongly on O sites to form hydroxyl but barely on the Ti_{5c} sites. The calculated adsorption energy (E_{ads}) on BBO (O_{2c}) and oxygen in the basal plane (O_{3c}) is −2.64 and −2.19 eV, respectively (Table 1, Fig. S9, ESI†). These values agree well with Yin et al's calculation results,[9d] suggesting that a H atom preferentially hydroxylates BBO sites on the stoichiometric rutile $TiO_2(110)$ surface. On the (2×2) rutile $TiO_2(110)$ surface with one BBO vacancy (θ_{Ov} = 0.25 ML), the adsorption energy of a H atom on

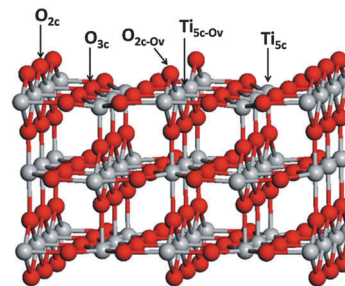
Fig. 5 Likely adsorption sites for atomic H on a (2×2) rutile $TiO_2(110)$ surface with one BBO vacancy (θ_{Ov} = 0.25 ML).

Table 1 Calculated adsorption energy (E_{ads}) of an atomic H on stoichiometric and defective (θ_{Ov} = 0.25 ML) rutile $TiO_2(110)$ surfaces

	Stoichiometric surface			Defective surface (θ_{Ov} = 0.25 ML)				
	O_{2c}	O_{3c}	Ti_{5c}	O_{2c}	O_{2c-Ov}	O_{3c}	Ti_{5c-Ov}	Ti_{5c}
E_{ads} (eV)	−2.64	−2.19	−0.07	−2.59	−2.47	−1.90	−2.44	−1.17

O sites is similar to the case of the stoichiometric surface, but the adsorption of a H atom with Ti_{5c} sites gets significantly enhanced (Table 1 and Fig. S10, ESI†). A H atom can bond with two Ti_{5c} sites beneath the BBO vacancy (Ti_{5c-Ov}) to form bridged H-Ti_{5c-Ov} species with an adsorption energy of −2.44 eV, which is as large as that on the BBO site. It can also adsorb on atop of a Ti_{5c} site in the basal plane to form atop H-Ti_{5c} species with an adsorption energy of −1.17 eV. The Co-adsorption energy of two H atoms on the defective surface was calculated to be roughly the sum of the adsorption energies of individual atomic H (Fig. S11, ESI†). These DFT calculation results demonstrate that stable hydride-type H-Ti species can form on the rutile $TiO_2(110)$ surface with surface oxygen vacancies exposed to atomic H, well supporting our experimental results.

The further Bader charge analysis results show that the H adatom in either bridged H-Ti_{5c-Ov} or atop H-Ti_{5c} hydride species bears a negative charge of −0.59 e. This demonstrates that partial charge transfer occurs from the defective rutile $TiO_2(110)$ surface to H adatoms on Ti sites. Reasonably negatively-charged H adatoms interact strongly with the positively-charged Ti site, forming stable H-Ti hydride species. Thus surplus electrons on the rutile $TiO_2(110)$ surface play an important role in the formation and stability of H-Ti species. Surplus electrons on the rutile $TiO_2(110)$ surface can be created by the formation of surface BBO vacancies as in our calculations, and also by the formation of surface hydroxyls via the adsorption of atomic H or molecular H_2 on O sites as in previous calculations.[9d,19]

Both experimental and DFT calculation results demonstrate the formation of stable photoactive hydride-type H-Ti species on the rutile $TiO_2(110)$ surface exposed to atomic H at 115 K. Therefore the γ and α H_2 desorption peaks in the TDS spectra that are affected by the UV light irradiation should arise from these H-Ti species. Correlating the desorption temperatures of γ and α peaks and the adsorption energies of atop H-Ti_{5c} and bridged H-Ti_{5c-Ov} species, we tentatively assigned the γ and α H_2 desorption peaks in the TDS spectra to surface reactions,

respectively, involving atop H-Ti$_{5c}$ and bridged H-Ti$_{5c\text{-}O_V}$. The β H$_2$ desorption peak that is not influenced by the UV light irradiation likely arises from surface hydroxyls that are not photoactive. Considering the DFT calculation results and the well-established reactivity of O$_{BB}$H, we tentatively assigned the β H$_2$ desorption peak to surface reaction involving O$_{3C}$H. The adsorption energy of atomic H on O$_{3C}$ is smaller than that on O$_{BBO}$, thus the surface reaction of O$_{3C}$H can occur at lower temperatures than that of O$_{BBO}$H.

Interestingly, the DFT calculation result that H-Ti species on the rutile TiO$_2$(110) surface are negatively charged suggests that the photocatalytic H$_2$ production from H-Ti species should be hole-mediated rather than electron-mediated. The rutile TiO$_2$(110) surface absorbs photons to excite electrons from the valence band to the conduction band and meanwhile generates holes in the valence band; then holes in the valence band migrate to the surface and oxidize H-Ti species to produce H$_2$. Such a hole-mediated photocatalytic H$_2$ production mechanism well explains the experimental observation of an obvious drop in the efficiency of photocatalytic HD and D$_2$ production with the increase of atomic D exposure from 20 to 50 L. The surface coverage of co-adsorbed water on the rutile TiO$_2$(110) surface increases greatly as the atomic D exposure increases from 20 K to 50 L (Fig. S3, ESI†). Zhang and Yates recently demonstrated effects of adsorbed molecules on the band bending of the rutile TiO$_2$(110) surface and the subsequent charge transportation processes from the bulk to the surface.[20] Adsorbed water on the rutile TiO$_2$(110) surface acts as an electron donor and thus causes the downward band bending, preventing excited holes from transporting from the bulk to the surface and decreasing the excited hole availability in the near surface region and subsequently the hole-mediated photocatalytic H$_2$ yield. It is noteworthy that a H-Ti species was reported to be abundant in the disordered layer of the black hydrogenated TiO$_2$ photocatalyst.[21] However, such a photo-excited hole-mediated H$_2$ production from H-Ti species over TiO$_2$ is not likely to be the mechanism for photocatalytic H$_2$ production from water that is photon-excited electron-mediated.

Conclusions

In summary we report for the first time photocatalytic H$_2$ production on TiO$_2$ model surfaces and identify negatively-charged hydride-type H-Ti species as the photoactive species. The formation and stability of H-Ti species are closely related to available surplus electrons on the rutile TiO$_2$(110) surface that can be created by the formation of surface BBO vacancies or by the formation of surface hydroxyls *via* the adsorption of atomic H or molecular H$_2$ on O sites. The photocatalytic H$_2$ production from H-Ti species is hole-mediated and co-existing water exerts a negative effect on this process. These results not only provide unprecedented fundamental understanding of photocatalytic H$_2$ production but also greatly broaden the photon-induced redox chemistry of TiO$_2$.

Acknowledgements

Notes and references

1 A. Fujishima and K. Honda, *Nature*, 1972, **238**, 37.

2 (*a*) T. L. Thompson and J. T. Yates, Jr., *Chem. Rev.*, 2006, **106**, 4428; (*b*) M. A. Henderson, *Surf. Sci. Rep.*, 2011, **66**, 185; (*c*) M. A. Henderson and I. Lyubinetsky, *Chem. Rev.*, 2013, **113**, 4428.

3 (*a*) J. T. Yates, Jr., *Surf. Sci.*, 2009, **603**, 1605; (*b*) N. G. Petrik and G. A. Kimmel, *J. Phys. Chem. Lett.*, 2010, **1**, 1758; (*c*) N. G. Petrik and G. A. Kimmel, *J. Phys. Chem. Lett.*, 2011, **2**, 2790; (*d*) Z.-T. Wang, N. A. Deskins and I. Lyubinetsky, *J. Phys. Chem. Lett.*, 2012, **3**, 102; (*e*) M. A. Henderson, M. Shen, Z.-T. Wang and I. Lyubinetsky, *J. Phys. Chem.*, 2013, **117**, 5774.

4 (*a*) A. Linsebigler, C. Rusu and J. T. Yates, Jr., *J. Am. Chem. Soc.*, 1996, **118**, 5284; (*b*) N. G. Petrik and G. A. Kimmel, *J. Phys. Chem. Lett.*, 2010, **1**, 2508; (*c*) M. C. Xu, Y. Gao, E. M. Moreno, M. Kunst, M. Muhler, Y. Wang, H. Idriss and C. Wöll, *Phys. Rev. Lett.*, 2011, **106**, 138302.

5 (*a*) B. Li, J. Zhao, K. Onda, K. D. Jordan, J. Yang and H. Petek, *Science*, 2006, **311**, 1436; (*b*) C. Zhou, Z. Ren, S. Tan, Z. Ma, X. Mao, D. Dai, H. Fan, X. Yang, J. LaRue, R. Cooper, A. M. Wodtke, Z. Wang, Z. Li, B. Wang, J. Yang and J. Hou, *Chem. Sci.*, 2010, **1**, 575; (*c*) C. Zhou, Z. Ma, Z. Ren, X. Mao, D. Dai and X. Yang, *Chem. Sci.*, 2011, **2**, 1980.

6 (*a*) M. Shen and M. A. Henderson, *J. Phys. Chem. Lett.*, 2011, **2**, 2707; (*b*) M. Shen and M. A. Henderson, *J. Phys. Chem. C*, 2012, **116**, 18788; (*c*) M. Shen, D. P. Acharya, Z. Dohnálek and M. A. Henderson, *J. Phys. Chem. C*, 2012, **116**, 25465.

7 (*a*) Q. Guo, C. Xu, Z. Ren, W. Yang, Z. Ma, D. Dai, H. Fan, T. K. Minton and X. Yang, *J. Am. Chem. Soc.*, 2012, **134**, 13366; (*b*) K. R. Phillips, S. C. Jensen, M. Baron, S.-C. Li and C. M. Friend, *J. Am. Chem. Soc.*, 2013, **135**, 574; (*c*) Q. Guo, C. Xu, W. Yang, Z. Ren, Z. Ma, D. Dai, T. K. Minton and X. Yang, *J. Phys. Chem. C*, 2013, **117**, 5293; (*d*) Q. Yuan, Z. Wu, Y. Jin, L. Xu, F. Xiong, Y. Ma and W. Huang, *J. Am. Chem. Soc.*, 2013, **135**, 5212.

8 (*a*) R. Nakamura, T. Okamura, N. Ohashi, A. Imanishi and Y. Nakato, *J. Am. Chem. Soc.*, 2005, **127**, 12975; (*b*) A. Imanishi, T. Okamura, N. Ohashi, R. Nakamura and Y. Nakato, *J. Am. Chem. Soc.*, 2007, **129**, 11569; (*c*) K. Onda, B. Li, J. Zhao, K. D. Jordan, J. Yang and H. Petek, *Science*, 2005, **308**, 1154; (*d*) S. Tan, H. Feng, Y. Ji, Y. Wang, J. Zhao, A. Zhao, B. Wang, Y. Luo, J. Yang and J. Hou, *J. Am. Chem. Soc.*, 2012, **134**, 9978.

9 (*a*) W. S. Epling, C. H. F. Peden, M. A. Henderson and U. Diebold, *Surf. Sci.*, 1998, **412/413**, 333; (*b*) S. Suzuki, K.-i. Fukui, H. Onishi and Y. Iwasawa, *Phys. Rev. Lett.*, 2000, **84**, 2156; (*c*) M. Kunat, U. Burghaus and C. Wöll, *Phys. Chem. Chem. Phys.*, 2004, **6**, 4203; (*d*) X.-L. Yin, M. Calatayud, H. Qiu, Y. Wang, A. Birkner, C. Minot and C. Wöll, *ChemPhysChem*, 2008, **9**, 253; (*e*) N. G. Petrik and G. A. Kimmel, *J. Phys. Chem.*, 2009, **113**, 4451.

7056 | *Phys. Chem. Chem. Phys.*, 2014, **16**, 7051–7057

This journal is © the Owner Societies 2014

10 (*a*) Y. Du, N. G. Petrik, N. A. Deskins, Z. Wang, M. A. Henderson, G. A. Kimmel and I. Lyubinetsky, *Phys. Chem. Chem. Phys.*, 2012, **14**, 3066; (*b*) C. Xu, W. Yang, Q. Guo, D. Dai, M. Chen and X. Yang, *J. Am. Chem. Soc.*, 2013, **135**, 10206.

11 G. H. Enevoldsen, H. P. Pinto, A. S. Foster, M. C. R. Jensen, W. A. Hofer, B. Hammer, J. V. Lauritsen and F. Besenbacher, *Phys. Rev. Lett.*, 2009, **102**, 136103.

12 J.-M. Pan, B. L. Maschhoff, U. Diebold and T. E. Madey, *J. Vac. Sci. Technol., A*, 1992, **10**, 2470.

13 (*a*) G. Kresse and J. Hafner, *Phys. Rev. B: Condens. Matter Mater. Phys.*, 1993, **47**, 558; (*b*) G. Kresse and J. Hafner, *Phys. Rev. B: Condens. Matter Mater. Phys.*, 1993, **48**, 13115; (*c*) G. Kresse and J. Hafner, *Phys. Rev. B: Condens. Matter Mater. Phys.*, 1994, **49**, 14251.

14 J. P. Perdew, K. Burke and M. Ernzerhof, *Phys. Rev. Lett.*, 1996, **77**, 3865.

15 W. Tang, E. Sanville and G. Henkelman, *J. Phys.: Condens. Matter*, 2009, **21**, 084204.

16 (*a*) L. Xu, Y. Ma, Y. Zhang, Z. Jiang and W. Huang, *J. Am. Chem. Soc.*, 2009, **131**, 16366; (*b*) L. Xu, W. Zhang, Y. Zhang, Z. Wu, B. Chen, Z. Jiang, Y. Ma, J. Yang and W. Huang, *J. Phys. Chem. C*, 2011, **115**, 6815; (*c*) L. Xu, Z. Wu, Y. Zhang, B. Chen, Z. Jiang, Y. Ma and W. Huang, *J. Phys. Chem. C*, 2011, **115**, 14290.

17 (*a*) W. Huang and W. Ranke, *Surf. Sci.*, 2006, **600**, 793; (*b*) W. Huang, W. Ranke and R. Schlögl, *J. Phys. Chem. B*, 2005, **109**, 9202; (*c*) W. Huang, W. Ranke and R. Schlögl, *J. Phys. Chem. C*, 2007, **111**, 2198; (*d*) B. Chen, Y. Ma, L. Ding, L. Xu, Z. Wu, Q. Yuan and W. Huang, *J. Phys. Chem. C*, 2013, **117**, 5800.

18 (*a*) J. Tao, Q. Cuan, X.-Q. Gong and M. Batzill, *J. Phys. Chem. C*, 2012, **116**, 20438; (*b*) M. L. Knotek, *Surf. Sci.*, 1980, **91**, L17.

19 J. Leconte, A. Markovits, M. K. Skalli, C. Minot and A. Belmajdoub, *Surf. Sci.*, 2002, **497**, 194.

20 (*a*) Z. Zhang and J. T. Yates, Jr., *J. Phys. Chem. Lett.*, 2010, **1**, 2185; (*b*) Z. Zhang and J. T. Yates, Jr., *J. Am. Chem. Soc.*, 2010, **132**, 12804.

21 X. Chen, L. Liu, P. Y. Yu and S. S. Mao, *Science*, 2000, **331**, 746.